Timescales of C turnover in soils with mixed crystalline mineralogies

Lesego Khomo[1], Susan Trumbore[1,2,], Carleton R. Bern[3], Oliver A. Chadwick[4]

[1]Max Plank Institute for Biogeochemistry, Germany
[2]Department of Earth System Science, University of California, Irvine, USA
[3]U.S. Geological Survey, Denver, CO, USA
[4]Department of Geography, University of California, Santa Barbara, USA

Correspondence to: Susan Trumbore (trumbore@bgc-jena.mpg.de)

Abstract. Organic matter-mineral associations stabilize much of the carbon stored globally in soils. Metastable short-range-order (SRO) minerals such as allophane and ferrihydrite provide one mechanism for long-term stabilization of organic matter in young soil. However, in soils with few SRO minerals and a predominance of crystalline alumino-silicate or Fe (and Al) oxyhydroxides C turnover should be governed by chemisorption with those minerals. Here we evaluate the role of different minerals on the amount and mean turnover time (TT) of C estimated from radiocarbon data in ancient soils sampled in Kruger National Park, South Africa. We measured ^{14}C in bulk soil, and fractions separated by density into free particulate and mineral-associated components. In parallel, we used chemical extractions of bulk soils to quantify Fe oxyhydroxides and SRO minerals. Because of our interest in the role of silicate clay mineralogy, particularly smectite (2:1) and kaolinite (1:1), we separately quantified the mineralogy of the clay-sized fraction using XRD and measured radiocarbon on the same fraction. Density separation demonstrated that 40–70% of bulk soil C for granites, nephelinite and dry gabbro soils and >80% in other soils was associated with minerals in surface soils. The parallel separation by size demonstrated that 9-47% of the organic C in these soils was strongly associated with clay-sized minerals. Organic C from surface soils strongly associated with this clay-sized fraction had mean TT averaging 1020 ± 460 years; more than 40% of the minerals identified in the same fraction were smectite (2:1 clays). The mean TT of C in this fraction increased with the amount of smectite it contained, indicating that 2:1 clays were associated with C of greater ages than the other mineral phases present in clay-sized material. Summed over the bulk soil profile, we found that smectite content also correlated with the mean TT of bulk soil C across varied lithologies. Thus, carbon strongly associated with smectite (2:1) clays can explain much of the variation in the age of soil C.

The carbon not strongly associated with clay-sized minerals includes a combination of low density C, C associated with minerals of size between 2µm and 2cm (including Fe oxyhydroxides coatings), and C removed from clay-sized material by 2% hydrogen peroxide. Based on mass balance, the TTs estimated for organic C in this fraction averaged 190±190 years in surface horizons.

SRO mineral content was generally very low in these soils (<0.5% by weight in all soils except those developed on gabbros under more humid climate). Soils with the most SRO had very high Fe and C contents, but surprisingly that C had short mean TT. In younger landscapes, SRO can be very stable and sorb Cover very long timescales. We hypothesize that in older landscapes SRO minerals are less stable, with that young C associated with them indicates that the minerals are short-lived. Across the varying lithologies and a precipitation gradient found in the KNP, we found Fe-oxyhydroxides (determined as the difference between Fe in dithionate citrate and oxalate extractions) to be the strongest predictor for soil C content. In contrast, mean TT of soil C was most related to the amount of smectite, whether measured in a single fraction (clay-sized material used for XRD mineralogy determination) or averaged over the whole soil profile. Combined with previous research on C turnover times in 2:1 versus 1:1 clays, our results hold promise for predicting C inventory and persistence based on intrinsic timescales of specific C-mineral interactions.

1 Introduction

The radiocarbon content of soil C provides a measure of how long C can persist in soils (Trumbore 2009). A working hypothesis is that the relative strengths of mineral-C interactions will be reflected in the radiocarbon content of the associated organic C. For example, 1:1 silicate clays with inherently low surface area, such as kaolinite, have limited sorptive capacity and retain C over relatively short timescales (Heckman et al., 2009; Sollins et al. 2009). In contrast, 2:1 clays with high charge density and high surface area, such as smectite, have higher affinity for C and thus retain it for relatively longer. In soils where the predominant minerals are smectites, organic C has older radiocarbon ages than in soils dominated by kaolinite (Wattel-Koekkoek et al., 2003; Poch et al., 2015). Soils in which much of the C is associated with high surface area short range order (SRO) minerals like Fe and Al oxyhydroxides contain organic C that has persisted for many millennia (Torn et al., 1997).

In soils of mixed mineralogy, several organic-mineral interaction mechanisms operate simultaneously, requiring multiple timescales for organic carbon persistence to explain radiocarbon measurements (e.g. Schrumpf and Kaiser 2014; Schrumpf et al. 2013; Wattel-Koekkoek and Buurman 2004).

The ability to quantitatively link specific mineral stabilization mechanisms with radiocarbon-based timescales of turnover is hampered because the operationally defined procedures used to quantify soil mineral content mostly differ from those used separate organic C into fractions that differ in radiocarbon content. Two main approaches are used to address this issue. One approach is to select samples for analysis from distinctly different global environments and use samples dominated by single mineral compositions (e.g. as described above; Wattel-Koekkoek et al. (2003)). Another approach is to sample soils along environmental gradients, and to correlate C age with the abundance of specific mineral stabilization mechanisms (e.g. Torn et al., 1997; Masiello et al., 2004; Lawrence et al. 2015), but often without full quantification of all the possible controls on C storage. Relatively few studies combine measures of the amounts and age of C in soil with quantitative measures of mineralogy. In particular, more studies

are needed that focus on the C stabilization behaviour of mature soils where long-term depletion of primary minerals and ripening of secondary minerals provides an environment dominated by well crystallized compounds that have relatively low chemical reactivity (c.f. Wattel-Koekoek et al., 2003; Torn et al., 1997). In regions with long-term tectonic and climatic stability, such as parts of the tropics and subtropics (Paton et al., 1995), it is possible that the differences in C sorption between 2:1 and 1:1 clays could be one of the most important controls on C storage and turnover.

Here we analyse a lithosequence of arid to subhumid savanna soils developed on the Kaapval Craton and associated post-Gondwana breakup lavas in Kruger National Park (KNP) South Africa (SA). Low rates of landscape erosion and exceptionally long soil residence times (Chadwick et al., 2013) ensure that nearly all soil minerals have evolved past the metastable SRO stage and that there are few free trivalent metal ions available for direct sorption by organic ligands (Khomo et al., 2011; Khomo et al., 2013). We evaluate ^{14}C in bulk soil, and fractions separated by density into free particulate and mineral-associated components. In parallel, we used chemical extractions of bulk soils to quantify Fe oxyhydroxides and SRO minerals, and quantified allied properties such as cation exchange capacity. Because of our interest in the role of silicate clay mineralogy, particularly smectite (2:1) and kaolinite (1:1), we separated the clay-sized fraction for XRD analysis of mineralogy, and measured radiocarbon on the same fraction.

Our specific research questions reflect the inherent limitations in combining different methods to quantify minerals and organic matter: (1) how do the amount and radiocarbon content of bulk, low density (<1.7 g cm^{-3}) and dense (> 1.7 g cm^{-3}) fractions vary among soils developed on different parent materials present in the Kruger National Park?; (2) can we define relationships between minerals and the amount and mean TT (derived from ^{14}C) of carbon?; and (3) can such relationships be extrapolated from specific soil samples to entire soil profiles and across soils with contrasting mineralogy? Our overall goal is to find relationships that allow us to predict the amount and TT of carbon across broader landscapes with similar soil forming factors.

2 Materials and Methods

2.1 Field sites

To evaluate mineralogical controls on C storage and turnover we sampled soils across gradients in geology, climate and topography in Kruger National Park (KNP). Soil residence times, estimated from average regolith depth and erosion rates determined using cosmogenic isotopes, are $>10^5$ yrs (Chadwick et al., 2013), providing ample time for crystalline mineral differentiation, ripening and depletion of metastable SRO minerals. In addition to strong geological differences across KNP, variation in clay mineralogy is imposed by a regional north-south gradient in rainfall that ranges from about 470 to 740 mm annually, and locally by differentiation of clay content along hillslopes. Under this setting, we can focus on

organic matter – mineral interactions associated with differences in silicate clays and secondary Fe and Al oxyhydroxides in an environmental regime expected to have few SRO minerals.

We sampled soils underlain by five geological units: rhyolite, granite, an olivine-rich picrite basalt (black basalt), an olivine-poor basalt (red basalt), and nephelinite (Venter et al., 2003) (Table 1, Figure 1). Each of the lithologies were sampled in the northern, arid zone, with mean annual temperature of 23 °C and ~470 mm annual precipitation. We also sampled soils developed on granite, gabbro and mixed granite/gabbro parent materials in the south of the park where rainfall ranges from ~550–740 mm per year (Table 1). Samples were collected along watershed divides, i.e. hill crests in the gently rolling landscape, although we include data for soils collected along one toposequence at 550 mm of rain to increase the amount of mineralogical differentiation that develops along granitic catenas in the KNP (Khomo et al, 2011; Khomo et al. 2013, Bern et al., 2011).

2.2 Bulk Soil Characterization

Soil profiles were sampled by horizon to bedrock where possible and described and classified using standard techniques. Soil depth ranged from 30 cm to about 2 m. Following air-drying, the samples were sieved to < 2 mm to remove rocks and roots. Air-dried samples were homogenized and sub-sampled for physical, chemical, isotopic and mineralogical analyses. Bulk density was measured as the mass of oven-dry soil in a core of known volume. The amount of clay-sized material (<2 μm size fraction) was determined by the hydrometer method (Soil Survey Staff, 2014). The concentration of exchangeable base cations was determined by atomic absorption spectroscopy after extraction with 1M ammonium acetate buffered at pH 7. Cation exchange capacity (CEC) was determined by extracting the ammonium saturated samples with a 1 M potassium chloride solution and determining ammonium by Lachat autoanalyzer. We report CEC corrected for the contribution of organic matter by assuming a contribution of 200 cmol(+) per kg organic C (as measured using an elemental analyser; Soil Survey Staff, 2014).

SRO minerals (aluminosilicate or Fe oxyhydroxides that are minimally polymerized) were extracted from bulk soils using acid ammonium oxalate (AAO) in the dark (Schwertmann, 1973). Iron (Fe(o)) and Al (Al(o)) from the extract were measured by Inductively Coupled Plasma-Optical Emission Spectrometry. We also applied a standard dithionite citrate bicarbonate (DCB) extraction and report the Fe concentration in this solution as Fe(d) (Mehra and Jackson, 1960). Total crystalline Fe oxyhydroxides are defined as Fe(d) – Fe(o). Carbon and nitrogen content were determined by combustion on a Vario Max CN elemental analyser. To determine if soils contained pedogenic soil carbonates, inorganic carbon was determined on the residue after dry combustion of bulk samples at 450 °C for 16 h (Steinbeiss et al., 2008) and organic carbon was calculated as the difference between total carbon and inorganic carbon. Carbonates were present in the red basalt and two of the dry gabbro profiles; carbonates in upper horizons were mostly present as individual particles (i.e. not coatings) presumably derived from more massive carbonates in a Bc horizon below.

2.3 Clay-sized material for XRD analysis

To isolate and prepare clay-sized material for XRD measurement of mineralogy, we started with bulk soil material. Sand-sized material was removed first by wet-sieving, and then the clay-sized (<2 μm) fraction for XRD was extracted following dispersion with 5% sodium hexametaphosphate and 2% H_2O_2, with three rounds of sedimentation and decantation in a 1L cylinder (Soil Survey Staff, 2014). The decanted material containing clay-sized material was evaporated and freeze-dried. The 2% H_2O_2 treatment, a standard pre-treatment for isolation of clay-sized material for XRD measurement, also removed organic C, and we waited for bubble formation (presumably from oxidation of organic matter) to cease before the first decanting procedure. Organic matter oxidized by this treatment included free particulate organic C, such as small plant fragments, that would also float in a solution of 1.7 g cm^{-3} (i.e. our low density fraction in 2.4 below). However, this treatment can also remove organic C that is weakly associated to clay-sized mineral surfaces. Thus we refer to material isolated this way as the "clay-sized XRD fraction" and assume that any C still in that fraction must be strongly associated with mineral surfaces. We estimate the C and C isotope content of C removed during isolation of the clay-sized XRD fraction using mass balance.

Splits of the clay-sized material were subjected to standard clay mineral identification routines including saturation with KCl and $MgCl_2$ before qualitative and quantitative analysis by X-ray diffraction (XRD). For mineral identification, peel-mounts of oriented clay-sized material were made by transferring the sample onto microprobe glass slides from 0.42 μm cellulose nitrate membrane filters where they had been oriented by vacuum (Pollastro, 1982). For mineral quantification, the clay-size fraction was micronized in methanol with 10% corundum by sample weight, dried, passed through a 50-μm sieve and placed into side-packed powder mounts (Eberl, 2003). XRD spectra were generated with a Siemens D500 diffractometer using Cu Kα radiation fitted with a graphite monochrometer configured to 35 mA and 40 kV. Mineral quantification was done using the Rockjock software (Eberl, 2003) and results were summed by mineral group. Additional mineralogy data for the clay-sized XRD fraction from select samples come from Khomo et al. (2011). All mineralogy data are normalized to sum to 100%.

2.4 Density Separation

For depth intervals identified as A horizons, where fresh plant inputs are largest, we performed a density separation on a sub-sample of soil. We used a heavy sodium polytungstate liquid (1.7 g cm^{-3}) to separate the sample into free light fraction (fLF) and heavy fraction (HF) (Schrumpf et al. 2013, modified to a density of 1.7 g cm^{-3}). A density of 1.7 g cm^{-3} is sufficient to separate minerals from fresh particulate organic material especially in soils with minimal SRO minerals that can have low densities (Castanha et al. 2007). Between 10 and 15 g of soil was added to 100 ml sodium polytungstate solution and gently shaken on a horizontal shaker for 10 min, ultrasonicated at 60 J ml-1 for 2.5 min, then centrifuged at 3500 rpm for 30 min. Because of the low energy used, we consider this fraction to be the "free" light fraction (fLF), i.e. there may still be some additional particulate material of low density trapped in aggregates that are not dispersed. The floating fLF was concentrated on filter paper (1.6 μm glass

microfiber discs) using a light vacuum. The sinking material was re-suspended in the heavy solution, and the steps repeated without the ultrasonic disaggregation until no more floating fLF was observed (usually three times). The fLF was rinsed with a litre of water to remove the heavy liquid, then freeze dried. Visible very fine roots were removed by hand (Castanha et al. 2007); coarser roots were removed by sieving previously, but the efficiency of these procedures varies, so we used the density separation to ensure all fine roots were removed from the sample. The remaining root-free fLF was ground to homogenize it for C isotope measurements. Somewhat lower C contents in the root-free fLF fraction in this paper (compared to other published studies that used different procedures) are likely due to removal of roots, combined with small amounts of mineral inclusion that were unavoidable as small-sized material was difficult to separate using the centrifuge (no flocculants were added).

We estimated the overall mass balance of the procedure by combining the mass and C contents of the different fractions (roots, root-free fLF and HF) with the mass and C content of the original bulk sample (Supplemental Table 1); in A horizons we lost 2-15% of the original C (Suppl. Table 2), likely through dissolution in the dense liquid (Castnha et al. 2007)

Thus, our analyses of C and radiocarbon in fractions contain overlapping information. For example, we can assume that all of the C and ^{14}C found in the clay-sized XRD fraction ($Clay_{XRD}$) is also found in the HF. The C removed during isolation of $Clay_{XRD}$, contains a mixture of C associated with minerals larger than clay-sized (e.g. a component of HF) as well as root and root-free fLF C (see also Results, Figure 4). While it would have been preferable to do a sequential extraction, the separation of sufficient clay-sized material for mineralogy and C isotope analyses from the HF fraction would have been costly and required large amounts of material (particularly for sandy soils with low clay content).

Similarly, our mineralogical information has some overlapping components. For example, in the $Clay_{XRD}$, we report Fe oxyhydroxides as the sum of minerals such as goethite, magnetite, maghemite and ilmenite (Supplementary Table 1). We do not normally refer to this fraction, but rather to the bulk soil measurement of Fe oxyhydroxides, which we define as the Fe compounds that are dissolved by a standard dithionite citrate extraction but not by the standard oxalate extraction (i.e. Fe(d) – Fe(o)). These compounds are assumed to be pedogenic Fe (though some amount of geogenic Fe is possibly also dissolved), and includes the $Clay_{XRD}$ Fe oxyhydroxides as well as coatings on minerals with sizes >2μm but <2mm.

2.5 Carbon isotopes

Radiocarbon (^{14}C) was determined by accelerator mass spectrometry (AMS). For determination of ^{14}C in organic samples, an amount of material (bulk soil, HF, fLF, or clay) needed to yield ~1 mg C was weighed into a pre-combusted quartz tube with CuO wire. The tube was evacuated, sealed with a torch and placed in a 900 ^{o}C furnace for 3 hours. The resulting CO_2 was purified on a vacuum line, and an aliquot was removed for determination of $^{13}CO_2$ using a gas bench coupled to an isotope ratio mass spectrometer (Xu et al. 2007). The remaining CO_2 was reduced to graphite using a sealed tube zinc reduction method (Xu et al. 2007), and isotopic compositions were measured at the WM Keck Carbon Cycle AMS facility at the University of California, Irvine. Samples which contained inorganic carbon were acidified with 1N HCl until the solution pH was

below 6 and then dried and analyzed as above. Carbonates were normally present as distinct sand-sized or larger grains, and were present only in the black basalt and the dry gabbro samples; we also used the ^{13}C signature of the combusted sample to indicate that carbonate did not contribute significantly to the measured sample C. For one soil, we analyzed ^{14}C in pedogenic carbonates by collecting and purifying the CO_2 evolved during acidification, then reducing it to graphite as for organic C samples.

Radiocarbon data are reported as $\Delta^{14}C$, the deviation from unity, in parts per thousand, between the ratio of ^{14}C /^{12}C in the sample divided by that of preindustrial wood (the standard). The potential influence of mass-dependent fractionation of isotopes is accounted for by reporting the ^{14}C /^{12}C ratio corrected to a common $\delta^{13}C$ value (-25‰), and assuming that ^{14}C is fractionated twice as much as ^{13}C by mass-dependent processes (Stuiver and Polach 1977). Therefore, differences in $\Delta^{14}C$ between samples reflect time or mixing rather than isotope fractionation. In these units, $\Delta^{14}C$ = 0‰ is equivalent to the standard. Values >0‰ indicate the presence of ^{14}C produced by atmospheric thermonuclear weapons testing in the early 1960s. Values <0‰ indicate that radiocarbon has had time to radioactively decay (half-life = 5730 years). Long-term accuracy for samples measured at the WM Keck CCAMS facility is ±3‰ for radiocarbon expressed as $\Delta^{14}C$ and ±0.1‰ for $\delta^{13}C$.

We also used the radiocarbon data to estimate the mean turnover time (TT) of soil C in the profile using a one-pool model that includes incorporation of bomb-^{14}C in the last decades and assumes steady state (see Torn et al. 1997; Trumbore 2009). Specifically, we used the SoilR package (Sierra et al. 2014) to calculate the predicted radiocarbon signature for such a one pool, steady state model in the year of sampling (R code used in included in Supplemental Material). For cases where two turnover times yielded the same ^{14}C in the year of sampling (for example, where $\Delta^{14}C$ is >0‰), we report both TT for the root-free fLF, but only the longer turnover time as more consistent with the fluxes of C into and out of the mineral associated and bulk fractions (see Gaudinski et al. 2000). The one-pool model is clearly an oversimplification, but is useful for translating radiocarbon data into average timescales of stabilization. The use of a mean TT also provides a way to compare data from samples collected in different years (2004–2011; Table 1). We want to emphasize that these TT only have meaning in the context of the assumptions used to generate them: they refer to C in a single, homogeneous pool at steady state.

We report carbon concentration and isotope data for individual horizons as well as whole-profile averages (e.g. as in Masiello et al., 2004). Mean carbon isotope ratios and mean estimated turnover times for whole profiles were calculated as averages, carbon-mass-weighted by horizon and calculated from measured bulk soil ^{13}C and ^{14}C values.

2.6 Statistics

Graphs, including regression analyses, were produced with R (R Core Team, 2015). Correlation matrices were produced using the R package Hmisc (Harrell et al. 2016). TT were calculated with the SoilR package (Sierra et al. 2014).

3 Results

3.1 Mineralogy

With few exceptions, these ancient soils contained low amounts (<0.3%, expressed as weight percent (g Fe/100g soil) of oxalate extractable Fe and Al presumed to be derived from SRO minerals (complete data are given in Supplemental Table 1). Only nephelinite-derived 0.5-0.9%) and sub-humid gabbro soils had greater (2.9%) concentrations of oxalate extractable Al+Fe. Crystalline Fe oxyhydroxides determined as Fe(d) – Fe(o) ranged from 0% in a periodically anoxic "seep" zone in the granitic toposequence to 5.2% in the nephelinite-soil.

The clay-sized XRD fraction made up ≤15% of the <2-mm mass for soils developed at crest positions on granites and rhyolites, but up to 35 - 50% in the red and black basalt, low rainfall gabbro and nephelinite soils, and at the toeslope of the granitic toposequence (Table 2; Suppl. Table 1). With a few exceptions, the amount of clay-sized material increased with soil depth.

Within the clay-size XRD fraction, the sum of smectite, kaolinite, micas and chlorite and crystalline Fe minerals generally made up over 90% of the quantified mineralogy (Table 2). Smectite was present in all of the isolated clays except the granite crest under relatively high (740 mm) rainfall, and dominated the clay fraction in red (>90%) and black basalts (>99%; Table 2). Kaolinite was common in most soils but rare in the arid zone gabbro and the two basalts. Crystalline Fe oxide minerals identified by X-ray diffraction made up 3-26% of the clay-sized fraction for most soils, but <1% in the smectite-dominated red and black basalts (Table 2).

Comparison of Fe oxyhydroxide abundance estimated by scaling quantitative XRD in the clay fraction to the whole soil (i.e multiplying the weight percent clay times the Fe oxide content measured by XRD) with that measured by extraction with DCB and oxalate in the bulk soil showed overall correspondence (see Supplemental Figure S1), but with much scatter. r

3.2 C in density fractions of A and B1 horizons

The root-free fLF isolated from A horizons had C concentrations of 10–37% (Table 3), with lower concentrations in the soils derived from rhyolite and the two basalts (10–16% C). As mentioned above, removal of roots and the inclusion of some clay-sized material during filtration can contribute lower values than expected if the root-free fLF is only fresh plant material. In general, carbon in the root free fLF made up only 10–20% of bulk C, even in surface soils (Suppl. Table 1). Mineral-associated heavy fraction (HF) had lower C concentrations but comprised more of the bulk soil mass, and represented 40–70% of bulk soil C for granites, nephelinite and dry gabbro soils and >80% in other soils (Table 3).

Root-free fLF $\delta^{13}C$ ranged from -24‰ to -14.5‰ (Table 3), reflecting a mixture of C3 and C4 vegetation sources. We found no relationship between root-free fLF $\delta^{13}C$ or HF $\delta^{13}C$ with rainfall, but mafic soils were consistently more enriched in $\delta^{13}C$ in both fractions compared to felsic

soils (Figure 2a). Radiocarbon signatures of root-free fLF (that includes char as well as plant fragments) varied from values close to those measured in annual grasses in 2010 (+35‰ in $\Delta^{14}C$) up to +145‰ (Figure 2b). For surface horizons, the one-pool model yielded two possible turnover times for most of the root-free fLF $\Delta^{14}C$. Assuming the shorter of the two for soil A horizons (normally 0–2 cm), yielded TT's from <1 to 8 years, while assuming the longer TT yielded 45–185 years (Table 3). For the black basalt and dry gabbro soil A horizons, only longer root-free fLF TT's (125–185 yrs) were consistent with observed $\Delta^{14}C$ signatures. TT of both root-free fLF and HF increased with depth. Fine roots picked from root-free root-free fLF in the red basalt soil had radiocarbon signatures equivalent to TT <1 year regardless of depth (Suppl. Table 1), and $\delta^{13}C$ signatures of -12 to -16‰.

The $\delta^{13}C$ of HF averaged ~ 3–4 ‰ more enriched than $\delta^{13}C$ of root-free fLF from the same soil (Figure 2a). Radiocarbon signatures in mafic soil HF were generally much more depleted in ^{14}C than root-free fLF from the same horizon (Figure 2b). Felsic soils tended to have higher ^{14}C values in HF than mafic soils, though this was less the case for root-free fLF fractions.

3.3 Changes in C, ^{13}C and ^{14}C with depth

Soil depths increased with rainfall from north to south. In all soils, C and ^{14}C concentration decreased with depth. Differences in lithology and hence mineralogy were more important controls on C and C isotopes than differences in rainfall (Figure 3 and Supplemental Table 2). Notably, soils developed on nephelinite had the highest C concentrations, while felsic soils had the lowest (Figure 3). Patterns in $\delta^{13}C$ by depth followed two general patterns. Felsic, gabbro and nephelinite soils had large (2–6‰) increases in between the surface and ~10–30 cm depth then became depleted below (Figure 3). Red and black basalt soils experienced a ~2‰ enrichment in $\delta^{13}C$ with depth and then stayed constant. Radiocarbon declined with depth in all soils, but in wetter sites (>550 mm annual rainfall) shifted towards higher ^{14}C values at the very bottom of the profile (BC or C horizons; Suppl. Table 1). The ^{14}C signatures of organic C in the red and black basalt soils was lower (<0‰ at all depths, even at the surface) compared to the other soils, and were the most enriched in $\delta^{13}C$ at all depths (Figure 3).

The B horizons of the red basalt and the two dry gabbro soils contained pedogenic carbonates at concentrations of up to several percent with radiocarbon ages ranging from ~4500–25000 ^{14}C years, substantially lower in ^{14}C compared to organic C at the same depths (see Suppl. Table 1). The carbonates in B1 horizons were generally found as distinct small but visible fragments (with ^{14}C ages up to ~4500 y) and likely derived from fragmentation and upward mixing of older and more massive carbonates deeper in the soil. Carbonates do not influence radiocarbon or signatures reported for organic matter in these soils as they were removed prior to combustion; the efficiency of removal can be observed in the similarity between isotope signatures of organic C in red basalts (containing carbonate) and black basalts (that did not have carbonate).

3.4 Carbon inventory and C strongly associated with clay-sized XRD fraction

The concentration of C strongly associated with the $Clay_{XRD}$- fraction ranged 1.0–4.7% across all soils Both the amount of C and its TT (ranging from 310-1330 years) increased with the amount of smectite measured in the same fraction (Table 4; Figure 5a). For $Clay_{XRD}$ samples where smectite made up >95% of the total mineral content, the mean TTs were in the range of 970-1250 years. C associated with $Clay_{XRD}$ samples where only ~45% of the mineral was smectites had the lowest TTs (340 years). We were unable to measure radiocarbon in samples from granites, due to the very low yield of clay-sized material in these soils.

Assuming bulk C has two components, a portion strongly associated with clay ($Clay_{XRD}$) and the rest of the soil C ("non-clay"), i.e. C that was removed with >2µm material (including coatings and organic matter associated with larger grains) or by the 2% H_2O_2 treatment (including much of the LF but also organic C weakly associated with clay sized material). We estimated the amount and radiocarbon signature of this "non-clay" component using mass balance:

$$\%C_{non\text{-}clay} = (\%C_{bulk} - F_{ClayXRD} \times \%C_{ClayXRD}) / (1 - F_{ClayXRD}) \quad (1)$$

$$\Delta^{14}C_{non\text{-}clay} = \Delta^{14}C_{bulk} - F_{ClayXRD} \times \Delta^{14}C_{ClayXRD}) / (1 - F_{ClayXRD}) \quad (2)$$

where $F_{clay\text{-}sized\ XRD}$ is the fraction of bulk-C that is found in the clay-sized XRD fraction:

$$F_{clayXRD} = (\%C_{clayXRDy} \times \%ClayXRD) / (\%C_{bulk} \times 100\%) \quad (3)$$

For the basalts, C in the $Clay_{XRD}$ fraction made up 40–47% of C_{bulk} in the top 2 cm, increasing to 80–86% in B horizons (see Suppl. Table 1). For all other soils, the amount of C strongly associated with $Clay_{XRD}$ accounted for <30% of bulk C. Other than the basalt-derived soils (and deeper B horizons in the gabbros; Suppl. Table 1), most bulk C was thus removed by the fractionation processes (size- and H_2O_2 treatment). As estimated from mass balance, the C removed ($\Delta^{14}C_{non\text{-}clay\text{-}sized}$) in the top 18 cm was (with one exception) dominated by C fixed in the last 50 years (Table 4). The estimated TT for non $Clay_{XRD}$ C ranged from 30-690 years, averaging 190±190 years; Table 4). The C strongly associated with $Clay_{XRD}$ (a fraction that includes not only clay minerals but up to 26% Fe oxides) for the same samples averaged 1020 ± 460 years.

As noted previously, the fractionation methods applied in this study, based on density and particle size, overlapped in what they measured (Figure 4). For example, all of the C in $Clay_{XRD}$ is a subset of HF. There is also overlap between the rfLF and the C removed when isolating $Clay_{XRD}$. The distribution of isotopes and C among the various fractions for one soil (illustrated as an example in Figure 4) demonstrate these variations and relationships, and show that the biggest differences in radiocarbon are between $Clay_{XRD}$ and rfLF fractionsE Fo.

Comment [1]:

3.5 Mineral – Carbon relationships at the profile scale

Profile-averaged properties were calculated to emphasize the factors that controlled differences between soils at scales larger than the soil horizon to highlight variation across the landscape (Table 5). This calculation introduced errors associated with highly uncertain estimates of gravel and bulk density (see values in Suppl. Table 1), but as these errors are identical for the elements being compared (e.g. profile-averaged concentrations), the profiles being compared should share systematic biases (i.e. similar operator error). The calculation of total profile C inventories (Table 5) are included to demonstrate the importance of these factors in understanding profile-scale C storage and dynamics. For example, the nephelinite soil had the highest C concentrations (averaging 3.8 %C for the whole profile) but was estimated to have 80–90% gravel (Supplemental Table 1), so the estimated C inventory (1.1 kg C m^{-2}) is not the highest when compared to other soils (which ranged from a low of 0.6 kg C m^{-2} in the dry granite soils to 11.4 kg C m^{-2} in the black basalt soils). Thus it should be remembered that the relationships derived here are for the <2-mm component of soil.

Mass-weighted mean profile $\%C_{organic}$ correlated significantly with mineral CEC (i.e. CEC corrected for organic matter contribution), and bulk Fe oxyhydroxides determined from Fe(d)-Fe(o) (Figure 6 and Suppl. Table 2). Together, bulk Fe oxyhydroxides and non-organic CEC explained most of the variation in carbon inventory across all soils. We found a significant relationship between the amount of smectite (determined as the % of mass in the clay-sized XRD fraction times the fraction of that mass that was quantified by XRD as smectite minerals) and the mean TT (Figure 6); total clay-sized XRD fraction and the fraction of smectite each also correlated individually with the horizon averaged bulk ^{14}C, but not as well as their product (see complete correlation matrix in Supplemental material, Table 2). The only highly significant correlation for bulk profile ^{13}C was with ^{14}C (Figure 6), though less significant correlations were found between ^{13}C and average clay content, and pH and CEC (Suppl. Table 2).

4 Discussion

Geological, climatic and topographic variation in Kruger National Park give rise to soils of varying mineral compositions. Different strengths of association of organic C with these minerals lead to observed patterns in C inventory and TT across the sampled landscape. None of the soil properties we measured showed a significant relationship with mean annual precipitation (Suppl. Table 2), indicating that any influence of climate on C amount and TT was indirect, through mineralogy and possibly vegetation. This was true even for the fractions, like rfLF, that are expected to be controlled by vegetation and climate. Underlying lithology significantly influenced the amount of clay-sized material, the amount of smectite in this material, cation exchange capacity and the TT of bulk C (Suppl. Table 2).

The mineral spectrum yielded by the broad environmental gradients sampled allowed us to determine whether there were simple, scalable relationships between measures of soil mineralogy with C amount and TT. Overall, we find that no single mechanism can explain both C inventory and TT, partly because our operationally defined fractions failed in most cases (all but the $Clay_{XRD}$ in basalts) to isolate pure mineral end members. We expected that in soils with low concentrations of SRO minerals, the ratio of smectite to kaoline would exert the strongest influence on C inventory and TT. We indeed observed that the C strongly associated with smectite minerals that made up >90% of the clay-sized minerals in basalts had TT averaging ~1000 years even in the top 2 cm, and overall the TT of C in the $Clay_{XRD}$ fraction correlated (weakly) with the amount of smectite (Figure 5a).

At the scale of the whole profile, the amount of smectite also correlated significantly with mean TT of C (Figure 5b). Hence, we conclude that the C strongly associated with smectite clay surfaces is responsible for the long TT of C in the clay-sized XRD fraction, and that the total amount amount of smectite clay in a soil profile exerts a control on the overall TT estimated from ^{14}C of bulk organic C. Soils at the toeslope of the granitic catena with HF C radiocarbon signatures +58‰ (i.e. TT of 130 yrs) still had 39–49% of their mass in the $Clay_{XRD}$ fraction. In that fraction, ~23–26% of the mass was identified as smectites and 53–57% as kaolin clay minerals; Table 2). This example demonstrates that it is not merely the amount of clay-sized material in the soil, but the amount of it that is smectite (i.e. 2:1 clay) that is key to long-term C storage in Kruger soils.

These results are in accord with findings by Wattel-Koekkoek and Buurman (2004) that C stabilized on smectite in surface horizons has turnover times of 600-1400 years in soils from Africa and South America. Wattel-Koekkoek et al. (2003) also showed that the older C associated with smectite tends to be more aromatic, suggesting that 2:1 clays provide a long-term store for fire-derived C. The aging of LF C with depth in fire-prone soils was shown to be related to the presence of char in soils from other fire-adapted ecosystems (Koarashi et al. 2013; Heckmann et al. 2009); where we analysed this in the red basalt soils in this study we found increased age of LF C with depth as well (Suppl. Table 1). Though we did not measure the chemistry of root-free fLF C, the presence of charred materials provides one possible reason for its low TT, particularly in the red and black basalts where grass biomass is high and fires frequent (Govender et al. 2006).

As is clear from our results, phyllosilicates provide just one mechanism for C storage in ancient soil. Given the very strong relationship between our bulk measure of crystalline Fe oxydroxides (i.e., Fe(d)-Fe(o)) and C concentration across our soils (Figure 6), it is reasonable to propose that Fe oxyhydroxides also provide important mechanisms for storing organic C, especially in soils with low smectite content. We cannot directly measure the TT of C removed by bulk extractions, due to the fact that both DCB and oxalate contain dissolved organic C. However, we can infer from the relatively short TT of C in soils with relatively smaller amounts of smectite minerals that the TT associated with the remaining mineral (kaolinite and Fe oxyhydroxides) is of the order of hundreds of years or shorter in A horizons. We thus expect millennial C associated with smectite to remain relatively insensitive to future changes in climate and land-use, while the decadal-centennial cycling C associated with the fLF, Fe oxyhydroxides and non-smectite clays like kaolinite should respond faster.

At the pedon scale, clay content was not the best predictor of the amount (r^2 =0.50, p=0.02) or TT (r^2 =0.59, p=0.03) of soil C, though this relationship improved when only smectite clay was considered (Figure 6; r^2 =0.75, p=0.001). Given the long TT associated with C stabilized by smectite, we conclude that even small addition of millennially-aged C strongly associated with smectite contributes substantially to the mean TT estimated from the bulk soil C. For example, mixing 75% C with a TT of 25 years with 25% C with a TT of 1200 years yields a bulk TT of ~320 years. Increasing the millenial pool to 35% changes the mean age of bulk C to ~450 years. The same is not true for C stocks, however, which are not significantly correlated with either clay (r^2 =0.50, p=0.08) or smectite clay (r^2 =0.45, p=0.12).

Somewhat unexpectedly, the subhumid gabbro and arid nephelinite soils with the highest concentration of SRO minerals (as determined from the Fe(o) and Al(o) extract concentrations), had younger C than would be predicted based on expected relationships between SRO minerals and C age found in other soils (c.f. Torn et al., 1997; Kramer et al., 2012). SRO minerals are particularly strong sorbers of C because their hydrated nano-crystals create intimate mixtures of mineral and organic material that - in the absence of drying and rewetting or redox pulses - tend to remain very stable (Chorover et al., 2004; Thompson et al., 2006b: Buettner et al., 2014). However, when SRO minerals are subjected to drying and rewetting or oxidation-reduction pulses, they reorganize into larger, more well-ordered crystalline compounds by ejecting C and water from the interior of their lattice structure (Ziegler et al., 2003; Thompson et al., 2006a). The wet gabbro and nephelinite soils had younger C, and only 9-17% of the C was associated with the clay-sized XRD fraction, even though they have >5% SRO mineral concentrations. The young C suggests that the SRO mineral phase is likely a relatively transitory phase that forms as primary minerals in the gravel and cobble fraction of the soil weather and ripen to kaolinite rapidly, with any C that was sorbed into the SRO mineral phase made available for microbial decomposition. In the same way, redox oscillations under seasonal wet-dry cycles promote crystallinity of Fe and we suggest that the Fe-bearing SRO minerals in these environments are likely short-lived giving way to crystalline Fe forms where C is sorbed to surfaces rather than within the less accessible lattice (Ziegler et al., 2003; Chorover et al., 2004). Thus, although the availability of a large surface area may promote stabilization of large amounts of C in these soils (e.g. nephelinite in Figure 3), the relatively rapid TT of that C may be a reflection of the short residence time of the minerals themselves and the short TT of C sorbed onto 1:1 clays and crystalline Fe oxyhydroxides. Studies of mineral-C interactions must consider not only the strength of C association with various mineral phases (e.g. strong for SRO and smectite, weak for kaolinite and oxyhydroxides)s, but also the timescale of mineral stability in the soil profile and pedogenic setting. Where SRO minerals and oxyhydroxides are stable, the associated C tends to be old, but in climates such as in Kruger the combination of a relatively short but strong rainy season and a long intervening dry season can lead to relatively rapid mineral transformation and hence rapid C turnover.

Factors that vary with soil depth exert controls on both C inventory and TT in KNP soils, as has been reported in many other areas. These affect the ^{14}C in all measured fractions. However, the rates at which age increased with depth differed between soils and C fractions. For soils with the largest amount of smectite clays (e.g. basalts), offsets in the TT for clay-sized XRD and the “non-clay-size” fractions were largest at the surface

and smallest at depth. In contrast, in soils with little smectite clay, the offset between fractions was relatively uniform with depth. More work is required to understand the stability of the different mineral phases themselves, especially organic C associated with Fe (and Al) oxyhydroxides phases, and how they interact with transport mechanisms in soil (e.g. Schrumpf et al. 2013; Schrumpf and Kaiser, 2015).

There appears to be a mineral/lithologic control on ^{13}C variation in KNP soils. This control can operate in at least two ways. First, the root-free fLF $\delta^{13}C$ seem to indicate greater C3-derived vegetation inputs to soils with more felsic parent materials, and a predominance of C4 inputs in more mafic soils (Figure 2a). This is consistent with the vegetation patterns on the ground (Scholes et al. 2003), with C4 grasses dominating the basalt soil landscapes. These patterns are largely preserved in the mineral-associated C (Fig. 2a), although HF $\delta^{13}C$ is consistently enriched compared to the LF $\delta^{13}C$. At the profile scale, the strongest predictor of $\delta^{13}C$ is $\Delta^{14}C$ (or TT; Fig. 6; r^2 =0.75, p=0.005), followed by pH (r^2 =0.65, p=0.016) and clay content (r^2 =0.65, p=0.017). For the isolated clay fraction, the relationship between $\delta^{13}C$ and smectite was weak. Soils with the greatest amount of smectite are also those with the greatest C4 vegetation, so it is unclear whether lithologic control on C3 versus C4 plants, or fractionation associated with different mineral stabilization mechanisms, is responsible for the overall trends observed in $\delta^{13}C$. Nonetheless, interpretations of paleo-vegetation from bulk soils must be undertaken with care, as variations in the mechanism of C stabilization across the landscape may affect the $\delta^{13}C$ signature as well as vegetation changes. More work is needed to disentangle these relationships at broader spatial scales encompassing climate and topographic gradients that will also involve changes in mineralogy.

Large parts of the land surface contain old soils with low concentrations of SRO minerals (Paton et al. 1995). We found good agreement in the age of C in the most smectite-rich (basalt soils) clay-sized XRD fraction, and those reported by Wattel-Koekek et al. (2003) from soils collected earlier at other sites in Africa and South America. Smectite clay content may thus provide a useful indicator for the fraction of C stabilized on millennial timescales over large areas. While quantitative clay mineralogy is not an easy measurement, the amount of smectite in our soils was broadly predictable from lithology and from more easily measured soil properties such as CEC (corrected for organic contributions), or pH (when below $CaCO_3$ saturation). Thus, across a range of landscapes and parent materials, one could predict how much of the C in soils is cycling on faster and slower timescales based on these parameters, while overall C inventory is more related to crystalline Fe and Al oxyhydroxides.

5 Conclusions

Differences in C cycling among soils differing in lithology, topography and rainfall are largely explained by varying mineralogy. Where SRO mineral concentration is low, the age of C in the clay-sized fraction depends on the concentration of smectite. However, this is only the case in basalts, for soils other than basalts, C TT averaged hundreds of years and is therefore weakly associated with the clay-sized fraction.

Our data indicate that heavy fraction C in old soils consists of two major components: a relatively 'passive' pool that stabilizes C for millennia that we suggest is strongly bound to smectite , and a more dynamic pool stabilized for decadal to centennial timescales that includes C bound to kaolinite and/or associated with crystalline Fe and Al (oxy)hydroxides. Most C in surface horizons, even in basalt soils where clays are >95% smectite, is in this faster-cycling pool. A small but highly dynamic light fraction pool also occurs across all soils. Increases in age of C with depth in soil profiles may indicate rates of vertical mixing or the time required for repeated sorption/release of C as it moves downwards, or it may reflect changes in the stability of the minerals themselves as a function of soil depth. While more research will be needed to understand these issues, our results hold great promise for predicting C inventory and TT based on intrinsic timescales of C stabilization mechanisms.

Acknowledgements

We thank two anonymous reviewers for constructive comments that improved the manuscript. This project was funded by grants from the Andrew W. Mellon Foundation to SET and OAC. We thank Ines Hilke and Birgit Frohlich for the CN analysis, Iris Kuhlman, Marco Pohlmann and others at the Max Planck Institute for Biogeochemistry for technical support. Thanks to South African National Parks for granting permission to work in the Kruger National Park and logistical facilitation, especially Patricia Khoza and Jacob Mlangeni. We thank Xioamei Xu and staff at the W. M. Keck Carbon Cycle Accelerator Mass Spectrometer, University of California at Irvine for radiocarbon data, and Jun Koarashi also helped with running samples at UC Irvine. William Benzel and George Breit provided invaluable assistance with mineralogical analysis. Shaun Levivk supplied the map for Figure 1. We thank Max for thought-garden space in SB and the following postdocs and graduate students at UCSB for insightful comments on an earlier version of the manuscript: Joseph Blankinship, Yang Lin, Eric Slessarev, Nina Bingham.

References

Bern, C.R., Chadwick, O.A., Hartshorn, A.S., Khomo, L.M. and Chorover J.: A mass-balance model to separate and quantify colloidal and solute redistributions in soil, Chemical Geology, 282(3–4), 113-119, 2011.

Buettner, S.W., Kramer, M.G., Chadwick, O.A. and Thompson, A.: Mobilization of colloidal carbon during iron reduction in basaltic soils, Geoderma, 221-222, 139-145, 2014.

Capo, R.C. and Chadwick, O.A.: Sources of strontium and calcium in desert soil and calcrete, Earth and Planetary Science Letters, 170, 61-72, 1999.

Carter, M. R.: Soil sampling and methods of analysis, Lewis Publishers, Boca Raton, 1993.

Castanha, C., Trumbore, S., and Amundson, R.G.: Methods of separating soil carbon pools affect the chemistry and turnover time of isolated fractions, Radiocarbon 50, 83-97, 2007.

Chadwick, O.A., Kelly, E.F., Merritts, D.J. and Amundson, R.G.: Carbon dioxide consumption during soil development, Biogeochemistry 24, 115-127, 1994.

Chadwick, O.A., Roering, J.J., Heimsath, A.M., Levick, S.R., Asner, G.P. and Khomo, L.M.: Shaping post-orogenic landscapes by climate and chemical weathering, Geology, 41, 1171-1174, 2013.

Chorover, J., Amistadi, M.K. and Chadwick, O.A.: Surface charge evolution of mineral-organic complexes during pedogenesis in Hawaiian basalt, Geochimica et Cosmochimica Acta 68, 459-476. 2004.

Eberl, D.D.:User's guide to RockJock, a program for determining quantitative mineralogy from powder X-ray diffraction data, U.S. Geological Survey Open-File Report 2003-78, 47p., 2003.

Gaudinski, J.B., Trumbore, S.E., Davidson, E.A. and Zheng, S.: Soil carbon cycling in a temperate forest: radiocarbon-based estimates of residence times, sequestration rates, and partitioning of fluxes, Biogeochemistry 51, 33-69, 2000.

Govender, N., Trollope, W. S., & Van Wilgen, B. W.: The effect of fire season, fire frequency, rainfall and management on fire intensity in savanna vegetation in South Africa, Journal of Applied Ecology, 43(4), 748-758, 2006.

Harrell, F.E., Jr, with contributions from Charles Dupont and many others.: Hmisc: Harrell Miscellaneous. R package version 3.17-2. https://CRAN.R-project.org/package=Hmisc, 2016.

Heckman, K., Welty-Bernard, A., Rasmussen, C. and Schwartz, E.: Geologic controls of soil carbon cycling and microbial dynamics in temperate conifer forests, Chemical Geology, 267(1), 12-23, 2009.

Kaiser, K. and Guggenberger, G.: The role of DOM sorption to mineral surfaces in the preservation of organic matter in soils. Organic Geochemistry 31, 711–725, 2000.

Khomo, L., Hartshorn,A.S., Rogers, K.H. and Chadwick,O.A.: Impact of rainfall and topography on the distribution of clays and major cations in granitic catenas of southern Africa, Catena, 87(1), 119-128, 2011.

Khomo, L., Bern, C.R., Hartshorn, A.S., Rogers, K.H. and Chadwick,O.A.: Chemical transfers along slowly eroding catenas developed on grantic cratons in southern Africa. Geoderma 202-203, 192-203, 2012.

Koarashi, J., Hockaday, W.C., Masiello, C.A. and Trumbore, S.E.: Dynamics of decadally cycling carbon in subsurface soils. JGR Biogeosciences 117, 2156-2202, 2012.

Kramer, M.G., Sanderman, J., Chadwick, O.A., Chorover, J. and Vitousek, P.M.: Long-term carbon storage through retention of dissolved aromatic acids by reactive particles in soil. Global Change Biology doi: 10.1111/j, 1365-2486, 2012.

Lawrence, C.R., Harden, J.W., Xu, X., Schulz, M.S. and Trumbore, S.E.: Long-term controls on soil organic carbon with depth and time: a case study from the Cowlitz River Chronosequence, WA USA. Geoderma 247-248, 73-87, 2015.

Liao, N.: Determination of ammonia by flow injection analysis. QuickChem Method 10-107-06-1-J., Lachat Instruments, Loveland, Colorado, 2001

Masiello, C.A., Chadwick, O.A., Southon, J., Torn, M.S. and Harden, J.W.: Weathering controls on mechanisms of carbon storage in grassland soils, Global Biogeochemical Cycles 18 (4), 2004.

Mehra, O. and Jackson, M.:, Iron oxide removal from soils and clays by a dithionite-citrate system buffered with sodium bicarbonate, Proc. 7th Nat. Conf. Clays., 1960.

Monreal, C.M., Schulten, H.R. and Kodama, H.: Age, turnover and molecular diversity of soil organic matter in aggregates of a Gleysol, Canadian Journal of Soil Science 77(3), 379-388, 1997.

Parfitt, R.L., and Childs, C.W.: Estimation of forms of Fe and Al - a review and analysis of constrating soils by dissolution and Mössbauer methods,Aust J. Soil Res. 26, 121-144, 1988.

Paton, T.R., Humphreys, G.S. and Mitchell. P.B.: Soils: A New Global View. Routledge, Taylor and Francis, New York, 1995.

Poch, O., Jaber, M., Stalport, F., Nowak, S., Georgelin, T., Lambert, J.F., Szopa, C. and Coll, P.:, Effect of nontronite smectitie clay on the chemical evolution of several organic molecules under simulated Martian surface ultraviolet radiation conditions. Astrobiology 15, 1-17, 2015

Pollastro, R.M.: A recommended procedure for the preparation of oriented clay-mineral specimens for x-ray diffraction analysis: Modifications to Drever's filter membrane peel technique. USGS Open-File Report 82-71, 24 p, 1982

R Core Team.: CorreR: A language and environment for statistical computing. R Foundation for Statistical Computing, Vienna, Austria. URL https://www.R-project.org/, 2015.

Scholes, R.J., Bond, W.J., Eckhardt, H.C.: Vegetation dynamics in the Kruger ecosystem. In: du Toit, J.T., Rogers, K.H., Biggs, H.C. (Eds.), Ecology and Management of Savanna Heterogeneity, Island press, Corvelo, 2003.

Schrumpf, M., Kaiser, K., Guggenberger, G., Persson, T., Kögel-Knabner, I. and Schulze, E. D.:Storage and stability of organic carbon in soils as related to depth, occlusion within aggregates, and attachment to minerals, Biogeosciences 10, 1675-1691, 2013.

Schrumpf, M. and Kaiser, K.: Large differences in estimates of soil organic carbon turnover in density fractions by using single and repeated radiocarbon inventories. Geoderma 239, 168-178, 2015.

Schwertmann, U.: Use of oxalate for Fe extraction from soils, Canadian Journal of Soil Science, 53(2), 244-246, 1973.

Sierra, C., Müller, M.M., Trumbore, S.E.: Modeling radiocarbon dynamics in soils: SoilR version 1.1, Geoscientific Model Development 7 (5), 1919-1931, 2014.

Soil Survey Staff.: Kellogg Soil Survey Laboratory Methods Manual. Soil Survey Investigation report No. 42, Version 5.0. R. Burt and Soil Survey Staff (ed.). US Department of Agriculture, Natural Resources Conservation Service, 2014.

Steinbeiss, S., Temperton, V. and Gleixner, G.: Mechanisms of short-term soil carbon storage in experimental grasslands, Soil Biology and Biochemistry 40(10), 2634-2642, 2008.

Stuiver, M. and Polach, H.: Reporting of 14C data. Radiocarbon 19, 355-363, 1977.

Thompson, A., Chadwick, O.A., Rancourt, D.G. and Chorover, J.: Iron-oxide crystallinity increases during soil redox oscillations, Geochimica Et Cosmochimica Acta 70(7), 1710-1727, 2006a.

Thompson, A., O.A. Chadwick, S. Boman, and J. Chorover. Colloid mobilization during soil iron redox oscillations. Environmental Science and Technology 40: 5743-5749. 2006b.

Torn, M.S., Trumbore, S.E., Chadwick, O.A., Vitousek, P.M. and Hendricks, D.M.: Mineral control of soil organic carbon storage and turnover, Nature 389(6647), 170-173, 1997.

Trumbore, S. E., Chadwick O. A. and Amundson, R.: Rapid exchange of soil carbon and atmospheric CO2 driven by temperature change, Science 272, 393-396, 1996.

USDA-NRCS.: Keys to Soil Taxonomy, United States Department of Agriculture, Lincoln, NE, 2010.

Venter, F.J., Scholes, R.J., Eckhardt, H.C.: The abiotic template and its associated vegetation pattern. In: du Toit, J.T., Rogers, K.H., Biggs, H. (Eds.), The Kruger Experience: Ecology and Management of Savanna Heterogeneity. Island Press, Washington, DC, pp. 83–129, 2003.

Wattel-Koekkoek, E. J. W., and Buurman, P.: Mean residence time of kaolinite and smectite-bound organic matter in Mozambiquen soils, Soil Science Society of America Journal, 68(1), 154-161, 2004.

Wattel-Koekkoek, E.J.W., Buurman, P., Van Der Plicht, J., Wattel, E. and Van Breemen, N.: Mean residence time of soil organic matter associated with kaolinite and smectite, European Journal of Soil Science, 54(2), 269-278, 2003.

Xu, X., Trumbore, S.E., Zheng, S., Southon, J.R., McDuffee, K, Luttgen, M. and Liu,, J.C.: Modifying A Sealed Tube Zinc Reduction Method for Preparation of AMS Graphite Targets: Reducing Background and Attaining High Precision, Nucl. Instr. and Meth. in Phys. Res. *B*, doi: 10.1016/j.nimb.2007.01.175, 2007.

Ziegler, K., J.C.C. Hsieh, O.A. Chadwick, E.F. Kelly, D.M. Hendricks and S.M. Savin.: Halloysite as a kinetically controlled end product of arid-zone basalt weathering. Chemical Geology 202: 461-478. 2003.

Table 1. Profile names used in the text, parent material lithology, mean annual precipitation (MAP), year of collection (Year), locations and classification of the soil profiles used for this study.

Profile name	Lithology	MAP (mm)	Slope Position	Year	Latitude (easting)	Longitude (northing)	Classification
GR-450-C	Granite	450	Crest	2004	322713	7452153	Haplocambid
GA-450-C	Gabbro	450	Crest	2010	321956	7449291	Calciustoll
RH-450-C	Rhyolite	450	Crest	2010	351375	7421676	Haplocambid
NE-450-C	Nephelinite	450	Crest	2010	336567	7398988	Ustorthent
BB-450-C	Black basalt)	450	Crest	2009	341888	7420588	Haplustert
RB-450-C	Red basalt)	450	Crest	2009	344120	7421754	Duritorrand
GR-550-C	Granite	550	Crest	2006	348678	7231971	Ustorthent
GR-550-S	Granite	550	Seepline	2006	348755	7231990	Dystrustept
GR-550-T	Granite	550	Footslope	2006	348831	7231986	Natrusalf
MG-550-C	Mixed granite	550	Crest	2010	341298	7232342	Ustorthent
MG-550-C2	Mixed granite	550	Crest	2010	341298	7232342	Ustorthent
GA-550-C	Gabbro	550	Crest	2005	333525	7230774	--
GA-740-C1	Gabbro	740	Crest	2010	329124	7218015	Haplotorrert
GA-740-C2	Gabbro	740	Crest	2010	329124	7218015	Haplotorrert
GR-740-C	Granite	740	Crest	2004	0326823	7211630	Dystrustept

Table 2. Mineralogy determined on clay-sized XRD fraction for selected soils (mostly mafic soils that had higher clay contents). Abbreviations: Q= Quartz, F= Feldspars, C= Calcite, O= Oxides, K= Kaolins, S=Smectites, Ch= Chlorites, M= Micas. Complete data can be found in Supplemental Table 1.

Identifier	Hor	Clay	Q	F	C	O	K	S	Ch	M
			----------% of clay-sized fraction ----------							
		(%)	-							
NE-450-C	A	30	1	1	0	15	24	47	0	12
NE-450-C	Bw1	40	1	1	0	14	26	48	0	9
BB-450-C	A1	39	1	0	0	0	6	92	0	0
BB-450-C	Bw1	43	2	0	0	0	5	93	0	0
RB-450-C	A1	36	1	0	0	0	0	99	0	0
RB-450-C	Bk2	46	2	0	0	0	0	98	0	0
GA-450-C*	A	15	2	2	0	7	0	67	0	22
GA-450-C*	Bw1	25	1	9	6	10	0	43	3	28
GA-740-C1	A	20	0	1	0	14	10	60	6	9
GA-740-C2	Bw1	25	0	1	0	8	16	68	6	1
GA-740-C3	Bw2	10	0	0	0	14	3	77	3	3
GR-550-C†	A	14	0	0	0	0	79	0	21	0
GR-550-C†	Bw2	17	0	0	0	0	79	1	21	0

GR-550-S†	A	6	0	0	0	0	76	17	7	0
GR-550-S†	Bw2	7	0	0	0	0	65	25	11	0
GR-550-T†	A	25	0	0	0	0	57	26	17	0
GR-550-T†	2Btn2	47	0	0	0	0	53	23	15	10

† Data are from Khomo et al. (2011).

Table 3. Carbon and carbon isotope signatures of heavy (HF, >1.7 g/cc) and root-free free light fraction (root-free fLF) carbon. Turnover times (TT) were estimated using the steady state, one pool model described in the text. When two TT were possible, we show both options for the root-freef LF fraction, but only the longer one for the HD fraction.

			Root-free fLF (free light fraction)				HF (Heavy fraction)			
Identifier	Depth (cm)	Total C in HF	C_{org} %	$\delta^{13}C$ ‰	$\Delta^{14}C$ ‰	TT yr	C_{org} %	$\delta^{13}C$ ‰	$\Delta^{14}C$ ‰	TT yr
GR-450-C	0-23	0.59	37.0	-23.7	99.3	5, 75	0.5	-19.5	30.1	195
	23-45	1.06*	24.6	-18.9	125.6	8, 50	0.4	-17.5	-35.9	510
GA-450-C1	0-2	na	34.2	-16.8	44.1	155	na	-13.6	6.2	275
	2-12	na	42.3	-15.0	34.4	180	na	-14.5	20.9	225
RH-450-C	0-3	0.81	16.6	-23.2	98.4	8, 75	0.7	-18.2	72.9	55
	3-15	0.83	1.9	-20.0	76.7	5, 100	0.5	-16.2	40.9	165
NE-450-C	0-2	0.65	31.3	-20.6	88.3	8, 85	4.2	-16.7	74.4	105
	2-18	0.76	30.8	-19.5	64.4	4, 120	2.4	-14.9	1.8	300
RB-450-C	0-4	0.82	11.6	-16.6	60.0	3, 125	1.8	-14.8	-23.1	425
	4-15	0.69	10.0	-16.6	30.0	195	1.4	-13.3	-95.2	985
	15-30	0.92	10.0	na	na	na	1.4	-13.3	-152	1560
	30-49	0.84	11.2	na	-53.0	330	1.3	-13.3	-216	2300
BB-450-C	0-3	n.d	10.0	-15.4	33.5	185	1.5	-13.7	-25.4	440
	3-11	0.78	7.5	-16.6	33.5	185	1.6	-12.9	-65.6	735
GR-550-C	0-15	0.70	16.0	-22.2	57.7	1, 130	0.5	-18.1	50.3	145
	15-41	na	14.5	-21.9	82.3	2, 95	0.4	-17.1	59.0	130
GR-550-S	0-2	0.72	22.5	-20.8	62.4	1, 120	0.5	-18.8	62.9	120
	2-10	1.1*	21.3	-20.2	82.1	4, 95	0.4	-19.1	96.1	80
GR-550-T	0-8	0.91	21.2	-18.0	54.7	1, 135	0.8	-16.7	58.0	130

	8-15	0.69	15.2	-19.9	74.4	105	0.5	-17.4	79.0	100
MG-550- C	0-3	0.84	36.9	-22.3	71.7	5, 125	0.9	-16.6	60.2	125
	3-10	0.92	15.5	-20.6	80.5	6, 110	0.7	-15.3	54.1	135
GA-550-C	0-9	na	29.9	-28.2	98.3	5, 85	2.8	-14.4	45.8	140
	9-24	na	15.2	-13.2	88	4, 100	2.3	Na	38.4	175
GA-740-C1	0-3	0.70	34.7	-16.9	72.6	1, 100	1.6	-13.4	78.2	100
	3-9	0.73	23.2	-14.8	40.5	165	1.5	-11.8	6.1	275
GA-740-C2	0-4	0.85	35.7	-16.1	67.6	4, 135	1.5	-13.1	85.2	90
	4-24	0.76	35.3	-16.9	64.4	4, 140	1.8	-12.8	60.6	125
GR-740-C	0-8	0.41	32.7	-21.3	145.8	10, 45	1.0	-16.8	143.9	45
	8-17	0.66	18.6	-17.8	95.0	4, 80	0.3	-15.1	109.4	70

* Values >1 indicate the magnitude of errors associated with density separations.

Table 4. Measurements of C and isotopes in the bulk soil and clay-sized XRD fraction, the same fraction analyzed for quantitative mineralogy (Table 2). The fraction of bulk C in the clay-sized XRD fraction ($F_{clayXRD}$) and the characteristics of the C making up the rest of the bulk C are calculated using equations 1-3, given in the text. Bottom depths >10 cm indicate B1 horizons; we excluded data from sampled depths >20 cm. We cannot rule out the potential for carbonates making up a small fraction of the $Clay_{XRD}$ fraction for the red basalt (RB-450-C) and dry gabbro (GA-450-C1) samples as these were not acidified prior to combustion for radiocarbon measurements; however, other soils did not contain carbonates, so are not affected.

	Bot.	Clay-sized (< 2-μm) XRD fraction				Bulk Soil					Remaining C ("non-clay")			
	Depth	C_{org}	$\delta^{13}C$	$\Delta^{14}C$	TT	Corg	$\delta^{13}C$	$\Delta^{14}C$	TT	$F_{clayXRD}$	C_{org}	$\delta^{13}C$	$\Delta^{14}C$	TT
Identifier	(cm)	(%)	‰	‰	(yr)	(%)	‰	‰	(yr)		(%)	‰	‰	(yr)
NE-450-C	2	2.52	-16.9	-1.5	310	6.04	-17.8	65.0	110	0.13	6.5	-17.9	69	110
NE-450-C	18	1.14	-16.8	-129.5	1330	3.04	-15.4	8.0	270	0.15	3.4	-15.3	16	240

GA-450-C1	2	4.69	-14.8	-64.6	730	3.28	-14.9	20.1	225	0.22	2.9	-14.9	58	130
GA-450-C1	12	2.35	-13.9	-145.0	1485	1.90	-13.9	-28.8	465	0.31	1.7	-13.9	43	160
RB-450-C	4	2.50	-14.1	-125.3	1275	1.94	-14.9	-16.0	385	0.47	1.5	-16.0	149	30
BB-450-C	3	2.48	-14.3	-91.7	955	2.41	-13.7	-25.4	440	0.40	2.4	-13.4	22	220
GA-450-C2	2	1.29	-16.3	-4.4	320	1.62	-16.6	22.0	220	0.12	1.7	-16.6	25	210
GA-740-C1	4	0.96	-17.6	-91.7	955	2.18	-11.8	-62.1	690	0.09	2.3	-11.6	-61	690
GA-740-C2	9	1.17	-19.1	-160.0	1650	1.76	-13.6	88.1	85	0.14	1.9	-12.9	122	55
GA-740-C2	24	1.10	-17.7	-116.1	1180	2.24	-13.4	70.0	110	0.10	2.4	-13.0	83	90

Table 5. Profile-averaged (excluding BC /C horizons) properties for the soils sampled in this study. Averages for C and C isotopes are calculated from bulk values. C inventory (Cinv) is the sum for the profile in kgC m^{-2}. All averages are mass-weighted, except C isotopes, which are weighted by the mass pf C in each horizon. Smectite content (Smec.) is estimated from multiplying the fraction of total mass in the clay-sized XRD times the %Clay (denoted in the table as Clay and expressed as per cent of total mass) by the percent of the clay-sized XRD identified as Smectite (Smec.; Table 2). Profile averaged values for ditionite citrate extracted iron (Fe(d)) and oxalate extractable iron Fe(o) and Aluminumn (Al(o)), as well as their difference, a measure of Fe oxyhydroxides in bulk soil, are all expressed as weight% as in mass Fe per 100 gram soil.

Identifier	Depth (cm)	Cinv	pH	CEC*	Clay (%)	Smec.	Fe_d	Fe_o	Fe_d - Fe_o	Al_o	C_{org} (%)	C/N	$\delta^{13}C$ (‰)	$\Delta^{14}C$ (‰)	TT (yr)
RH-450-C	30	1.3	6.8	5.5	1.0	10	2.7	0.1	2.6	0.1	0.66	9.9	-16.2	28.0	230
GR-450-C	23	0.6	6.1	7.7	6.3	46	0.6	0.0	0.6	0.0	0.78	11.9	-20.2	30.4	200
NE-450-C	18	1.1	6.8	61.8	38.7	48	5.4	0.3	4.9	0.2	3.85	11.8	-15.9	9.9	235
BB-450-C	49	11.4	7.7	44.3	42.0	98	1.7	0.2	1.5	0.2	1.56	14.2	-13.5	-140.4	1500
GA-450-C	34	8.6	8.3	25.7	9.9	50	1.9	0.2	1.7	0.2	1.66	na	-15.0	-37.0	550
RB-450-C	70	8.6	7.0	50.1	46.2	93	2.5	0.1	2.4	0.1	1.53	14.8	-12.3	-156.4	1720
GR-550-C	62	3.5	5.4	3.2	14.8	1	0.4	0.1	0.3	na	0.32	21.2	-15.3	12.2	430
GR-550-S	41	1.8	5.1	2.6	7.5	21	0.1	0.0	0.1	na	0.23	19.6	-18.6	51.8	150
GR-550-T	46	3.6	7.0	29.9	42.7	24	0.2	0.1	0.1	na	0.50	14.1	-14.7	24.8	225
MG-550-C	38	2.6	6.9	7.8	15.0	41	1.4	0.3	1.1	0.2	0.82	14.2	-13.8	-68.6	755
GA-740-C1	44	7.0	7.2	37.7	17.7	69	2.6	1.1	1.5	0.4	1.53	12.2	-13.9	-47.5	250
GA-740-C2	25	4.5	7.3	31.5	25.8	25	2.5	2.0	0.5	0.3	1.49	11.9	-13.3	26.9	150
GR-740-C	93	5.1	5.7	7.0	3.7	**10**	0.4	0.0	0.4	0.0	0.36	14.8	-18.5	88.8	240

Depth indicates the depth to which the in the profile averages were calculated (we excluded BC and C horizons).

Values in bold for smectite content (Smec.) were not measured but are assumed based on similar lithology values. We assumed average values for the horizons above and/or below to fill in data for smectite content for depths in a profile where no measurements were available (see Supplemental information).

Subscripts d and o represent dithionite and oxalate extracts for Fe and Al.

Figure 1. Locations and lithology of parent materials where soils were sampled for this study. Rainfall decreases from ~740mm/a in the southern end of the park to ~450 mm/a in the northern end of the park.

Deleted:

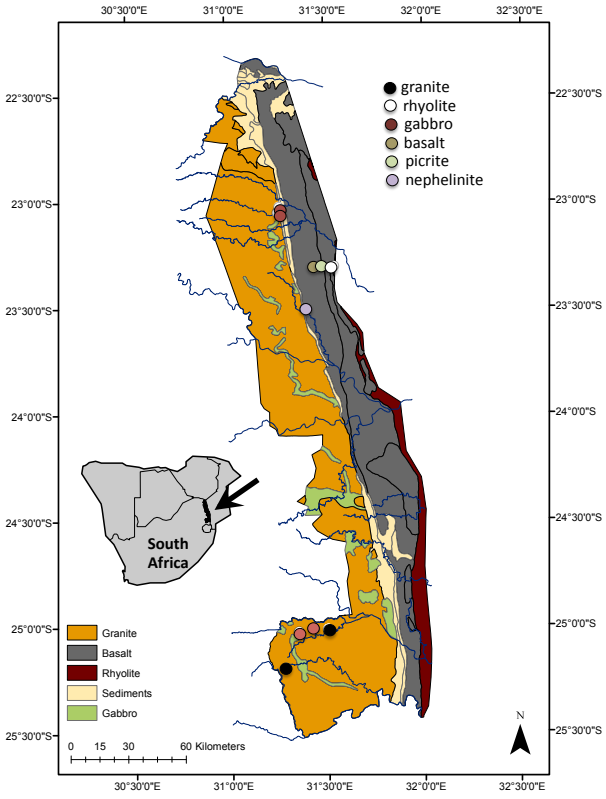

5

Figure 2. Comparison of ^{13}C (2A) and ^{14}C (2B) in root-free free light fraction (root free-fLF) and heavy fraction (HF) organic C for individual samples from A horizons (see Table 3). Felsic lithologies (open circles) include soils developed on granite and rhyolite, mafic lithologies (filled circles) include soils developed on gabbros and basalts and nephelinite. The 1:1 correlation line is plotted for reference.

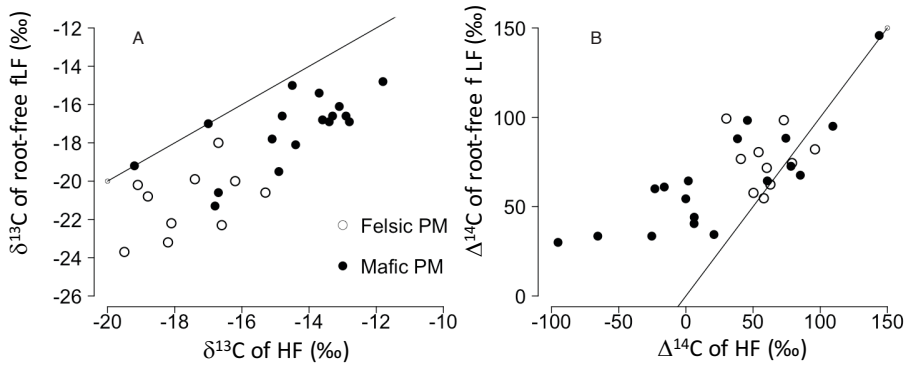

Figure 3. Depth profiles of bulk C (top-left), and the $\delta^{13}C$ (top-middle), and $\Delta^{14}C$ (top-right) measured in bulk C for soil profiles developed on selected lithologies. Also shown in the lowr panel are other soil bulk properties, total Fe oxyghroxides (Fe(d)- Fe(o)) (bottom-left), total nitrogen (bottom middle) and cation exchange capacity (CEC) corrected for organic matter contributions (see text; bottom right).

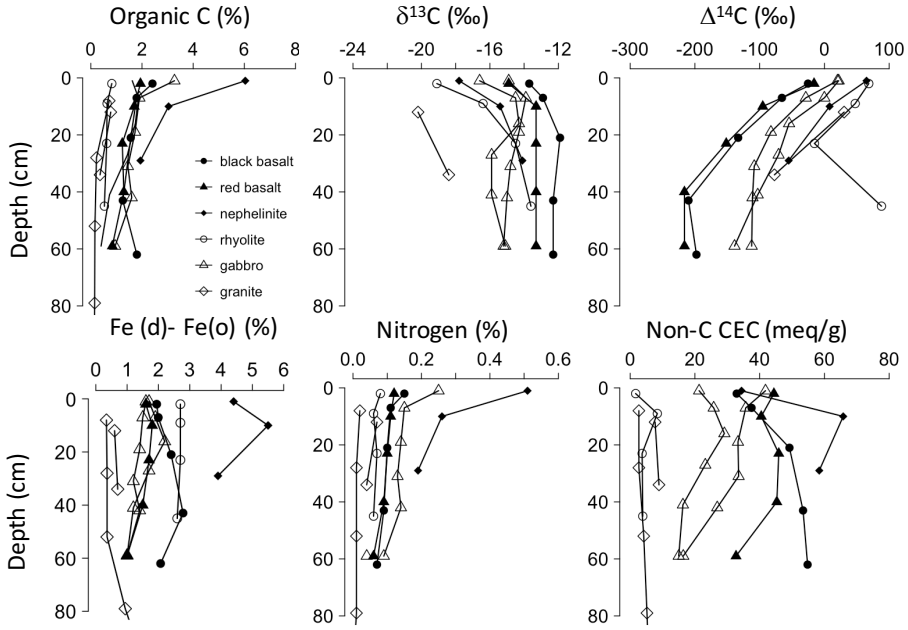

Figure 4. Comparison of C and C isotopes for a single soil sample (0-3 cm depth in GA-740-C (gabbro parent material) indicating the inter-relationships among the different process-defined organic C fractions. For each fraction we indicate the percent of total C (C_T) it contains; fractions for root-free fLF and HF do not add to 100% because of contributions from roots picked from the free ligh fraction (fLF) and C that dissolves in the polytungstate solution and is not recovered. Colors indicate overlaps between C among different fractions exist. For example, C strongly associated with the clay-sized fraction measured with XRD ($Clay_{XRD}$; orange) makes up part of the HF-C. Free low density C (fLF; light green, including both roots picked from the fLF and the root-free fLF fractions) makes up part of the non-clay-sized fraction. Most of the fLF is likely removed from the $Clay_{XRD}$ when it is treated with 2% H_2O_2.

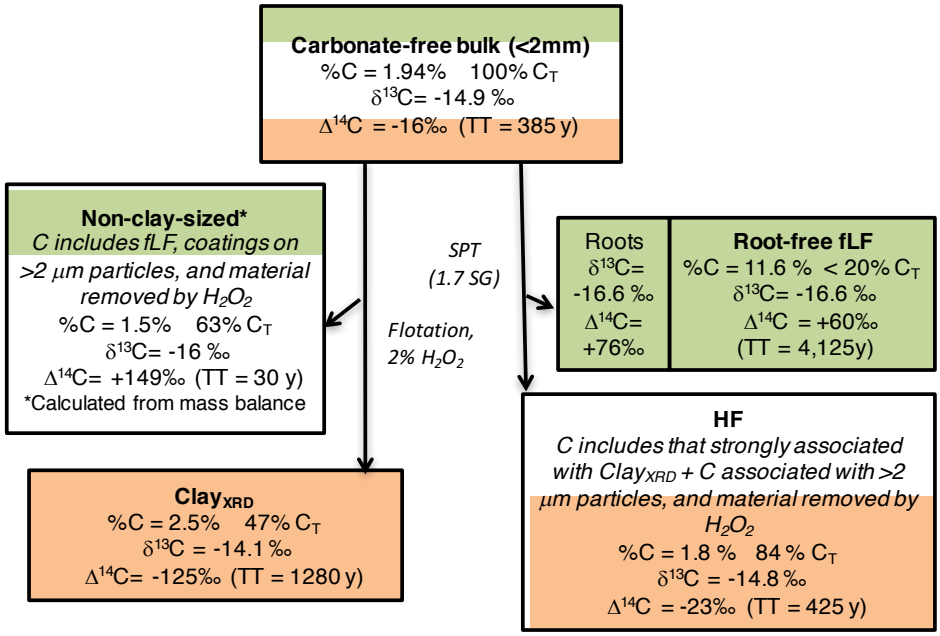

Figure (left). Mean Turnover Time (TT) of C in the clay-sized XRD fraction increases with smectite concentration, the linear relationship for A horizon points (n=7) has R-squared =0.48 and p=0.08. (Right) Mean TT of bulk C averaged for each profile compared to the fraction of the total C that is found in the clay-sized fraction ($F_{clayXRD)}$. The mean TT of bulk organic C correlates significantly with the fraction of organic matter strongly associated with the clay-sized XRD fraction. Here the linear relationship R-squared = 0.54 and p=0.004

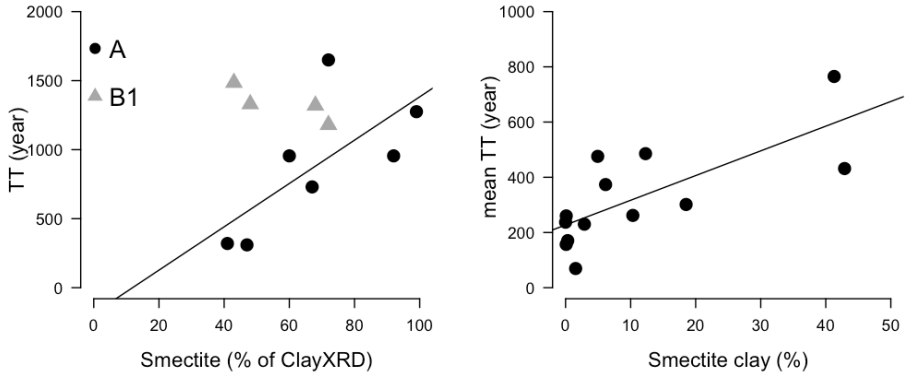

Figure 6. Across all the studied soils, the mean %C in the soil profile was best predicted by Fe(d)-Fe(o) (left; R-squared = 0.60, p=0.003), and cation exchange capacity (right; R-squared = 0.63, p=0.0003). The best predictors for profile-averaged C turnover times was the amount of smectite clay (Figure 5 (right)). Correlation matrices for other variables in Table 5 are given as Supplemental Table 2.

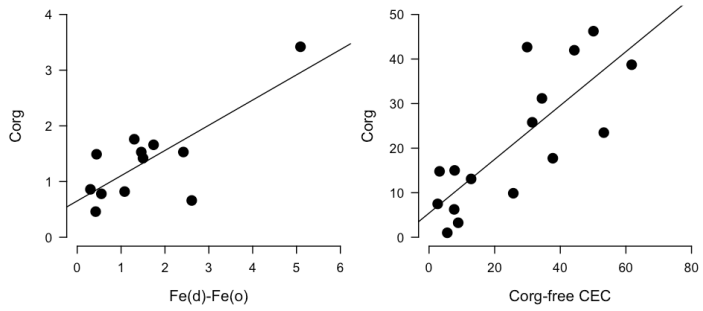
Corg
Fe(d)-Fe(o)
Corg
Corg-free CEC